3750–3767 Nucleic Acids Research, 2014, Vol. 42, No. 6 Published online 13 January 2014
doi:10.1093/nar/gkt1359

The light-induced transcriptome of the zebrafish pineal gland reveals complex regulation of the circadian clockwork by light

Zohar Ben-Moshe[1,†], Shahar Alon[1,2,†], Philipp Mracek[3], Lior Faigenbloom[1], Adi Tovin[1], Gad D. Vatine[1], Eli Eisenberg[2,4], Nicholas S. Foulkes[3] and Yoav Gothilf[1,2,*]

[1]George S. Wise Faculty of Life Sciences, Department of Neurobiology, Tel-Aviv University, Tel-Aviv 69978, Israel, [2]Sagol School of Neuroscience, Tel-Aviv University, Tel-Aviv 69978, Israel, [3]Institute of Toxicology and Genetics, Karlsruhe Institute of Technology, Eggenstein-Leopoldshafen 76344, Germany and [4]Raymond and Beverly Sackler School of Physics and Astronomy, Tel-Aviv University, Tel-Aviv 69978, Israel

Received November 4, 2013; Revised December 6, 2013; Accepted December 9, 2013

ABSTRACT

Light constitutes a primary signal whereby endogenous circadian clocks are synchronized ('entrained') with the day/night cycle. The molecular mechanisms underlying this vital process are known to require gene activation, yet are incompletely understood. Here, the light-induced transcriptome in the zebrafish central clock organ, the pineal gland, was characterized by messenger RNA (mRNA) sequencing (mRNA-seq) and microarray analyses, resulting in the identification of multiple light-induced mRNAs. Interestingly, a considerable portion of the molecular clock (14 genes) is light-induced in the pineal gland. Four of these genes, encoding the transcription factors *dec1*, *reverbb1*, *e4bp4-5* and *e4bp4-6*, differentially affected clock- and light-regulated promoter activation, suggesting that light-input is conveyed to the core clock machinery via diverse mechanisms. Moreover, we show that *dec1*, as well as the core clock gene *per2*, is essential for light-entrainment of rhythmic locomotor activity in zebrafish larvae. Additionally, we used microRNA (miRNA) sequencing (miR-seq) and identified pineal-enhanced and light-induced miRNAs. One such miRNA, miR-183, is shown to downregulate *e4bp4-6* mRNA through a 3′UTR target site, and importantly, to regulate the rhythmic mRNA levels of *aanat2*, the key enzyme in melatonin synthesis. Together, this genome-wide approach and functional characterization of light-induced factors indicate a multi-level regulation of the circadian clockwork by light.

INTRODUCTION

Intrinsic circadian oscillators driving daily rhythms of physiology and behavior evolved as an adaptation to the 24-h solar cycle (1). At the molecular level, the vertebrate circadian clock is based on transcriptional and translational auto-regulatory loops that generate oscillations of clock genes and their protein products (2). In the primary feedback loop are the positive components, CLOCK and BMAL, that heterodimerize and activate transcription of target genes, including *period* (*per*) and *cryptochrome* (*cry*), through E-box enhancer elements. Negative feedback is accomplished by PER:CRY heterodimers that re-enter the nucleus and repress their own transcription by inhibiting the CLOCK:BMAL complex (3). The robustness and accuracy of this core loop is achieved by stabilizing accessory feedback loops and post-translational regulation (3,4). Nevertheless, the intrinsic period length of the circadian clock deviates from 24 h and therefore requires daily synchronization by environmental time-cues, among which light is the most dominant (5). Changes in gene expression within central clock structures is thought to be one of the processes required for light-entrainment, but what exactly these changes are and how they lead to light-entrainment is yet to be defined.

The zebrafish serves as an attractive vertebrate model for exploring the central circadian clock and its entrainment by light (6). As in other non-mammalian vertebrates, the zebrafish pineal gland incorporates all the elements required for light-entrainment and circadian rhythm generation and is considered to serve as a master clock organ; it is photoreceptive and contains an intrinsic circadian oscillator that controls the rhythmic production of the hormone melatonin (7). Furthermore, most zebrafish tissues and even cell lines possess peripheral clocks that can be entrained by direct light exposure (8). This differs

*To whom correspondence should be addressed. Tel/Fax: +972 3 640 6329; Email: yoavg@tauex.tau.ac.il

†These authors contributed equally to the paper as first authors.

from the case in mammals, in which the retina is the source of photic input to the clock, and the peripheral clocks are entrained indirectly by the master oscillator that is located in the suprachiasmatic nucleus (SCN) of the hypothalamus (9). Accordingly, the zebrafish pineal gland and zebrafish cell lines constitute a suitable platform for studying the molecular mechanisms of the circadian clock and its entrainment by light.

Light-induced gene expression constitutes a key element in the relay of photic information to the core clock machinery. In zebrafish, light exposure triggers the transcription of *per2* and *cry1a* in most tissues and in cell lines, a process which is thought to underlie the entrainment of the circadian clock (10,11). Systematic promoter analyses of these clock genes identified D-box as a key *cis*-acting element in the regulation of light-driven gene expression (12,13). Transcriptome analyses in zebrafish embryos (14), larvae, heart and cell cultures (15) demonstrated light regulation of various cellular processes, such as transcriptional control and DNA-repair, using microarray technology. These studies have contributed to the understanding of light-regulated gene expression in peripheral clock-containing tissues. Nevertheless, a comprehensive understanding of light-entrainment requires investigation of light-induced gene expression in the central clock organ. Moreover, high-throughput messenger RNA (mRNA) sequencing (mRNA-seq) now offers improvements in the profiling of the light-induced transcriptome, mainly due to unlimited gene representation and generation of enhanced quantitative data (16).

With the aim of further unraveling the mechanisms underlying light-entrainment of the vertebrate central circadian clock, we used both mRNA-seq and microarray technologies to characterize the light-induced transcriptome in the zebrafish pineal gland. Focusing on light-induced genes that encode transcription factors (*dec1*, *reverbb1*, *e4bp4-5* and *e4bp4-6*), we demonstrated their effects on clock- and light-regulated promoter activation. Among these factors, we showed that *dec1*, as well as the core clock gene *per2*, is important for the light-entrainment of rhythmic locomotor activity. Light-induced genes generally exhibit a transient increase in expression, pointing to the existence of mechanisms that govern mRNA stability, such as regulation by microRNA (miRNA). Accordingly, we used miRNA sequencing (miR-seq) to identify miRNAs whose expression is enhanced in the pineal gland and induced by light. We demonstrated that the pineal-enhanced and light-induced miR-183 regulates *e4bp4-6* mRNA levels through a target site in its 3′UTR. Moreover, we showed that miR-183 contributes to the generation of rhythmic mRNA levels of the pineal clock-controlled gene, *aanat2*. Overall, the genomic approach and functional analyses indicate a complex regulation of the central circadian clock by light.

MATERIALS AND METHODS

mRNA-seq, miR-seq and microarray experimental procedures

Adult (0.5–1.5-year-old) Tg[*aanat2*: enhanced green fluorescent protein (EGFP)] zebrafish (17) were raised in a temperature-controlled re-circulation water system under 12-h: 12-h light–dark (LD) cycles, and transferred to constant darkness (DD) at the end of the day before the experiment. Fish were exposed to a 1-h light pulse ('daylight' fluorescent lamp, light intensity of 5 W/m^2) before sampling (light treatment) or kept under constant darkness for control (dark treatment). The fish were anesthetized in 1.5 mM Tricane (Sigma) and sacrificed by decapitation. Pineal glands and brains were removed and immediately processed within 3 min of dissection under an Olympus dissecting microscope SZX12 equipped with filters for excitation (460–490 nm) and emission (510–550 nm) of EGFP; the use of transgenic fish expressing EGFP in the pineal gland enabled its selective removal. The tissues were collected from light- and dark-treated fish at six time points with 4-h intervals throughout one daily cycle, corresponding to circadian times (CT) 2, 6, 10, 14, 18 and 22 (Figure 1).

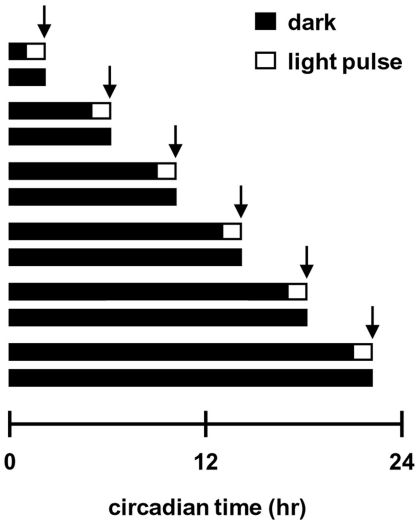

Figure 1. Experimental design for transcriptome analysis. Horizontal bars represent the photic treatments preceding tissue sampling: groups of fish were exposed to a 1-h light pulse (white boxes) or kept in darkness (black boxes), and tissues were sampled immediately after the treatment at six circadian time points indicated by arrows.

For microarray analysis, 12 pineal glands were collected and pooled at each time point under both light and dark treatments. For mRNA-seq, pineal glands were collected at the six sampling times and pooled together to establish triplicates of 15 pineal glands for every treatment. For miR-seq, 18 pineal glands were pooled from the six sampling times for both light and dark treatments, and one brain pool was composed of four brains that were collected from light- and dark-treated fish at CT2 and CT14. Brain samples were collected subsequent to the removal of pineal glands and therefore do not contain pineal tissues. Total RNA for mRNA and miRNA analyses was isolated using RNeasy Lipid Tissue Mini Kit (Qiagen) and miRNeasy Mini Kit (Qiagen), respectively. The sequencing data were deposited to the Sequence Read Archive, under accession SRP016132. The microarray data were deposited to the Gene Expression Omnibus, under accession GSE53288.

mRNA-seq and data analysis

The Illumina TruSeq protocol was used to prepare libraries from RNA samples. Overall, six libraries (three light groups and three dark groups) were run on one lane of an Illumina HiSeq2000 machine using the multiplexing strategy of the TruSeq protocol (Institute of Applied Genomics, Italy). On average, ~6.7 million paired-end reads were obtained for each library. The reads were of 2×100 bp. TopHat (18) was used to align the reads against the zebrafish genome, keeping only uniquely aligned reads with up to two mismatches per read. Different pair-end reads with identical start positions in the genome in both pairs might represent polymerase chain reaction (PCR) duplicates (19); therefore, in these cases, only one representative pair-end read was included. Only reads that are aligned to the protein coding regions of known NCBI reference sequence (RefSeq) genes were used. A custom script written in Perl was used to parse the output of TopHat, given in Sequence Alignment/Map format (http://samtools.sourceforge.net/), and to convert it into raw number of reads aligned to each position in each RefSeq gene. The RefSeq genes information was obtained from the Table Browser of the UCSC genome browser (genome.ucsc.edu/) using the zebrafish July 2010 (Zv9/danRer7) assembly. On average, ~10% of the reads passed all filters and were mapped to coding regions of RefSeq genes.

Statistically significant differences between the number of reads aligned to each RefSeq gene (the expression profile) in the different tested conditions were identified as described (20). Briefly, the expression profiles were normalized using a variation of the trimmed mean of M-values normalization method (20,21). Subsequently, we searched for expression differences between the three dark samples and the three light samples that cannot be explained by the expected Poisson noise with $P < 0.05$ and Bonferroni correction for multiple testing (20).

miR-seq and data analysis

miRNA capturing and library construction for the pineal light, pineal dark and brain samples were conducted using Illumina's TruSeq Small RNA Sample Prep Kit according to the manufacturer's protocol. The mature miRNA libraries were sequenced with bar-codes on one lane of an Illumina HiSeq2000 instrument following the manufacturer's protocol. The reads were filtered using Illumina's HiSeq2000 software. The total number of reads after filtering was ~6, ~10.4 and ~14.8 million for the pineal light, pineal dark and brain, respectively. Next, the reads were aligned against the zebrafish genome, as described (22), providing ~4, ~5.8 and ~4.3 million reads for the pineal light, pineal dark and brain, respectively. Approximately 3.8, ~5.4 and ~3.5 million reads were aligned to known miRNAs [miRBase, release 17; (23)] for the pineal light, pineal dark and brain, respectively.

All the expression profiles of the mature miRNAs were normalized, and statistically significant differences between the profiles were identified as indicated above for the mRNA-seq and as previously described (20). For the comparison between the expression levels in the pineal and in the brain, a minimum fold change of 2 was required in addition to the above.

Microarray and data analysis

Labeled RNA preparation and hybridization to DNA microarrays were performed according to the Affymetrix manual with the two-cycle target labeling protocol (http://www.affymetrix.com/support/downloads/manuals/expression_analysis_technical_manual.pdf). A total of 12 Affymetrix DNA microarrays were hybridized with RNA-pools of pineal glands from light and dark treatments in six time points throughout the daily cycle. Each DNA microarray was normalized using Affymetrix GeneChip Operating Software. The entire DNA microarray data set, logarithmically transformed, was normalized using quantile normalization to guarantee that the distribution of probe intensities was the same in all the chips (24).

The identification of transcripts with significantly different expression levels in the light and dark groups was performed as follows: (i) The sum of differences in expression levels between the light and dark groups was plotted against the transcripts average log expression for all transcripts represented in the DNA microarray, along with a moving average trend line. Logarithmically transformed microarray data are highly variable at low expression levels, mainly due to the background (additive) noise (25). As a consequence, a moving average trend line is higher for low average expression. (ii) Each transcript was given a z-score, measuring how far is its sum of differences from the trend line, compared with the standard deviation of all the sum of differences of transcripts with a similar expression level. A high z-score for a given transcript indicates that the variation in the expression levels is higher than the variation expected from the transcript average expression level. The specific z-score used as a detection cutoff was chosen to keep the associated false-positive rate at 5%. The false-positive rate for a given z-score was calculated by assuming a normal distribution for the transcripts expression levels, and accordingly, for the sum of differences in expression levels. Transcripts with low expression values (i.e. their mean expression level over all time points is lower than the average of all transcripts) in both the light and dark groups were discarded. This analysis was performed for all six time points, yielding a list of 16 genes. To avoid misdetection of genes due to inaccuracy in a single microarray measurement, the analysis was also performed for every five consecutive time points, yielding 13 additional genes (Supplementary Table S1).

Gene Ontology analysis

The 92 pineal gland light-induced genes that were detected by mRNA-seq (Table 1) were subjected for gene enrichment analysis using the DAVID functional annotation tool (26). The DAVID's default zebrafish genes background was used. Significantly enriched ontology terms (Benjamini–Hochberg false discovery rate of 5%) are listed in Supplementary Table S2.

Validation of light-induced gene expression by whole-mount *in situ* hybridization

Wild-type zebrafish embryos were entrained by two 12-h: 12-h LD cycles and transferred to DD. On the third day of

Table 1. Pineal gland light-induced genes detected by mRNA-seq

Number	Gene symbol	RefSeq ID	L/D-fold	Number	Gene symbol	RefSeq ID	L/D-fold
1	*pfkfb4l*	NM_198816	5.09	47	*rtn4rl2a*	NM_203479	2.28
2	*rtn4rl2b*	NM_203483	4.92	48	*vsnl1a*	NM_001007366	2.26
3	*nr4a3*	NM_001172629	4.81	49	*si:ch211-195b13.1*	NM_001077302	2.25
4	*pvalb7*	NM_205574	4.81	50	*insig1*	NM_199869	2.23
5	*nr1d1 (reverba)*	NM_205729	4.79	51	*hif1al*	NM_200405	2.22
6	*stmn4l*	NM_001002563	4.61	52	*znf238*	NM_001082952	2.21
7	*tagln2*	NM_201576	4.51	53	*stk35*	NM_001077616	2.2
8	*nppcl*	NM_001161341	4.38	54	*eng2a*	NM_131044	2.2
9	*mibp*	NM_131693	4.26	55	*bactin1*	NM_131031	2.17
10	*zgc:122979*	NM_001037574	4.09	56	*ifrd1*	NM_001076555	2.12
11	*fkbp5*	NM_213149	3.99	57	*hivep2*	NM_001030164	2.1
12	*jun*	NM_199987	3.77	58	*pik3r3b*	NM_201143	2.09
13	*bhlhe40 (dec1)*	NM_212679	3.6	59	*trim9*	NM_205563	2.05
14	*lonrf1l*	NM_001277234	3.59	60	*hsd11b2*	NM_212720	2.05
15	*osbpl7*	NM_001005927	3.54	61	*nfil3-5 (e4bp4-5)*	NM_001197058	2.03
16	*cnn2*	NM_213349	3.41	62	*glulb*	NM_182866	2.02
17	*nfil3-6 (e4bp4-6)*	NM_001002218	3.36	63	*zgc:63637*	NM_213365	2.02
18	*klf9*	NM_001128729	3.35	64	*dennd4a*	NM_001080989	2.01
19	*itm2cb*	NM_199980	3.32	65	*ppm1nb*	NM_001103117	2
20	*gabrb2*	NM_001024387	3.29	66	*coch*	NM_001003823	1.99
21	*per1a*	NM_001030183	3.29	67	*camk4*	NM_001017607	1.96
22	*slc20a1a*	NM_213179	3.28	68	*camk2n1*	NM_001145089	1.96
23	*tuft1a*	NM_001080001	3.1	69	*snap25a*	NM_131435	1.95
24	*per2*	NM_182857	3.07	70	*midn*	NM_207052	1.95
25	*cry1a*	NM_001077297	3	71	*chac1*	NM_001110126	1.94
26	*tmem178*	NM_001076640	2.99	72	*ucp2*	NM_131176	1.91
27	*nfil3-2 (e4bp4-2)*	NM_001197065	2.97	73	*scn8aa*	NM_131628	1.91
28	*camk2d2*	NM_001002542	2.89	74	*cyp27c1*	NM_001113337	1.9
29	*dbpb (dbp2)*	NM_001197062	2.87	75	*nrxn1a*	NM_001080021	1.78
30	*sptlc2b*	NM_001114741	2.75	76	*myl9b*	NM_213212	1.74
31	*pim3*	NM_001034978	2.71	77	*rpe65a*	NM_200751	1.73
32	*tgfbi*	NM_182862	2.7	78	*slc17a7*	NM_001098755	1.68
33	*jund*	NM_001128342	2.57	79	*tef1*	NM_131400	1.67
34	*bhlhe41 (dec2)*	NM_001039107	2.54	80	*grk7a*	NM_001031841	1.6
35	*mid1ip1*	NM_213439	2.54	81	*nr1d2b (reverbb2)*	NM_131065	1.6
36	*npas4a*	NM_001045321	2.52	82	*neurod*	NM_130978	1.58
37	*gfap*	NM_131373	2.51	83	*cplx4a*	NM_001077300	1.55
38	*speg*	NM_001007109	2.5	84	*stmn2a*	NM_001005923	1.54
39	*cry3*	NM_131786	2.48	85	*atp1a1b*	NM_131690	1.53
40	*nr1d2a (reverbb1)*	NM_001130592	2.45	86	*atp1b1a*	NM_131668	1.45
41	*abcf2*	NM_201315	2.4	87	*diras1*	NM_199831	1.44
42	*zgc:154093*	NM_001077731	2.36	88	*stxbp1*	NM_001025182	1.43
43	*arg2*	NM_199611	2.34	89	*atp2b2*	NM_001123238	1.41
44	*c1qtnf4*	NM_001017702	2.33	90	*gpm6aa*	NM_213200	1.4
45	*camk2b1*	NM_001271393	2.29	91	*gpm6ab*	NM_214687	1.37
46	*zgc:153615*	NM_001077791	2.28	92	*zic2a*	NM_131558	1.28

development, embryos were exposed to a 1-h light pulse ('daylight' fluorescent lamp, light intensity of 5 W/m^2) at six time points (CT2, 6, 10, 14, 18 and 22); control embryos remained in darkness. The collected embryos were fixed and subjected to whole mount *in situ* hybridization (ISH) followed by quantification as previously described (11,27). DNA fragments from the coding regions of *dec1*, *e4bp4-6*, *per1a*, *reverbb1*, *pfkfb4l* and *lonrf1l* were PCR amplified, cloned into pGEM T-Easy vectors (Promega) and served as templates for generation of anti-sense riboprobes using DIG RNA labeling kit (Roche). PCR amplification was conducted using the primers listed in Supplementary Table S3A. For each transcript, validation of light-induction by whole-mount ISH was conducted at two selected circadian time points. Differences between treatments were determined by two-tailed *t*-test.

Validation of light-induced gene expression by quantitative real-time PCR

Adult Tg(*aanat2*:EGFP) zebrafish were exposed to light and dark treatments as described in the section 'mRNA-seq, miR-seq and microarray experimental procedures' above, resulting with three pools of six pineal glands per treatment under six sampling times. Total RNA was extracted using RNeasy Lipid Tissue Mini Kit (Qiagen), and cDNA was prepared using High-Capacity cDNA Reverse Transcription Kit (Applied Biosystems). Quantitative real-time PCR (qRT-PCR) analysis was carried out by absolute quantification using ABI PRISM 7300 Sequence Detection System (Applied Biosystems), according to the manufacturer's protocol. Triplicates of light and dark cDNA samples from selected time points served as templates for PCR amplification using SYBR Green PCR

Master Mix (Applied Biosystems) and specific primers (Supplementary Table S3B). Expression levels were normalized to *beta-actin2* (*bactin2*) transcript, and differences between treatments were determined by two-tailed *t*-test. Light-induction of every transcript was assayed by qRT-PCR at two circadian time points.

Transient transfections of Pac-2 cells and live-cell bioluminescence assays

Pac-2 cells (28) were cultured as described (29) and transiently transfected using the FuGene HD reagent (Roche Diagnostics) according to the manufacturer's protocol. Promoter reporter constructs: *per1b-Luc* contains 3.3 kb of *per1b* promoter region cloned into luciferase expression vector pGL3Basic [Promega, (30)]; *cry1a-Luc* consists of a fragment of 1.3 kb encompassing 1.25 kb of the 5′ flanking and 53 bp of *cry1a* first exon, cloned into pGL3Basic (12); *E-box*$_{per1b}$*-Luc* contains four copies of the *per1b* E-box (5′-GAAGCACGTGTACTCG-3′) cloned into the minimal promoter luciferase reporter vector pLucMCS [Stratagene, (30)]; *D-box*$_{per2}$*-Luc* contains six copies of the *per2* D-box (5′-TGCGTCTTATGTAAAAAGAG-3′) cloned into pLucMCS (13); and *AP-1-Luc* reporter construct, consisting of four copies of the canonical *cry1a* AP-1 #1 site (5′-TGACTCA-3′) cloned into pLucMCS (12). The coding sequences of selected transcription factors were incorporated into CMV promoter-driven expression vectors: *dec1* and *reverbb1* were cloned into pcDNA3.1 (Invitrogen); *e4bp4-5* and *e4bp4-6* were cloned into pCS2-MTK [derivative of pCS2, (31)]. Empty expression vectors served as negative controls. Transiently transfected cells were exposed to three LD cycles and two 24-h periods under DD conditions, and live-cell bioluminescence assays were carried out as described elsewhere (13,30) using a Topcount NXT counter (2-detector model, Perkin Elmer). Traces represent the mean of four independently transfected wells ± SD from a single experiment. Each experiment was performed a minimum of two times. Peak and amplitude values (Supplementary Table S4) were calculated as in previous studies (13,32). Briefly, short-term and long-term trends were removed from the raw data by an adjacent-averaging method with 4-h and 5-day running means, respectively, providing 'luciferase activity values'. Normalized values were obtained by dividing the luciferase activity values by their average value. The peak was calculated as the highest point of the normalized values on the third LD cycle. The amplitude was computed as the difference between the normalized luciferase activity of the peak and the preceding trough, divided by 2. Statistical differences were determined by two-tailed *t*-test.

Morpholino-mediated knockdown in embryos

Knockdown experiments were performed using morpholino-modified antisense oligonucleotides (MO, Gene Tools): Gene Tools standard control MO (5′-ctcttacctcagttacaatttata-3′); per2$_{(E4I4)}$MO (5′-tgcagatgtacttacagtgtttttg-3′) designed to target the splice site between exon 4 and intron 4, resulting in aberrant *per2* splicing (33); dec1$_{(E2I2)}$MO (5′-aattacgcattcgtaccttactgtc-3′) targeting the exon 2 and intron 2 boundary to interfere with *dec1* splicing; and miR-183$_{(guide)}$MO (5′-acagtgaattctaccagtgccatac-3′), designed to target dre-miR-183 guide strand and block its activity. One-cell stage embryos were injected with MOs (2 nl, 1 mM) and incubated under different lighting regimens as indicated. The efficiency of per2$_{(E4I4)}$MO and dec1$_{(E2I2)}$MO targeting splice sites was evaluated by RT-PCR ensuring the formation of altered transcripts throughout the locomotor activity monitoring period [5–8 days post-fertilization (dpf)]. Total RNA was extracted from injected embryos, and cDNA was synthesized as previously described (33). Transcripts were PCR-amplified using the primers listed in Supplementary Table S3C.

Larval locomotor activity assays

Embryos injected with control MO, per2$_{(E4I4)}$MO or dec1$_{(E2I2)}$MO, were transferred within 4 h post-fertilization (hpf) to a temperature-controlled incubator at 28°C and maintained under constant darkness for four days. On the fifth day, larvae were placed in 48-well plates in the observation chamber of the DanioVision Tracking System (Noldus Information Technology), entrained by 3-h light (LED, light intensity of 1.8 W/m^2) and transferred to constant dim light conditions (LED, light intensity of 0.013 W/m^2) for four daily cycles. Locomotor activity was tracked and analyzed by the Ethovision 8.0 software (Noldus Information Technology). Tracks from days 6–8 were analyzed for the total distance moved (cm) by each larva per 10 min time-bins. The data are presented as a moving average (20 sliding points) of ~24 larvae in each group. To determine alterations in rhythmic locomotor activity, individual tracks underwent Fourier analysis as previously described (34,35). Briefly, the time-dependent signals were converted to frequency-dependent signals using the Fast Fourier Transform and scored with a ratio ('G-factor') representing the extent to which the frequency corresponds to a 24-h period. Differences in the G-factor distributions between control MO- and per2$_{(E4I4)}$MO- or dec1$_{(E2I2)}$MO-treated groups were determined by the Kolmogorov–Smirnov test.

Profiling light-induction of mRNA in Pac-2 cells by quantitative real-time PCR

Pac-2 cells were exposed to three 12-h: 12-h LD cycles. Subsequently, total RNA was extracted from cells kept in darkness or exposed to light [tungsten light source, 0.2 W/m^2, as previously described (12)] for different time periods (0.5, 1, 1.5, 2, 3, 4, 6 and 8 h). Total RNA was isolated using Trizol reagent (Gibco BRL), and cDNA was transcribed using SuperScript III reverse transcriptase (Invitrogen) with random primers. qRT-PCR was conducted using TaqMan Gene Expression Assays (Applied Biosystems). PCR reactions were carried out using the ABI PRISM 7300 Sequence Detection System (Applied Biosystems) with TaqMan Universal PCR Master Mix (Applied Biosystems) according to the manufacturer's instructions. Expression levels were calculated by the $2^{-\Delta\Delta CT}$ method relative to *bactin2*. Values are the mean

of three independent cell pools. Differences between photic treatments and sampling times were determined by two-way analysis of variance (ANOVA). TaqMan pre-designed primer and probe sets (Assays-on-Demand, Applied Biosystems) were used for *dec1* (assay ID: Dr03101060_g1) and *per2* (assay ID: Dr03093705_m1). Custom TaqMan (Assays-by-Design, Applied Biosystems) was used to determine the expression of *e4bp4-5*, *e4bp4-6*, *cry1a* and *bactin2* with primers and probe sequences as presented in Supplementary Table S3D.

Transient transfections and dual luciferase assays in HEK-293T cells

The constructs used for transient transfections of HEK-293T cells were prepared as follows. *psiCHECK-aanat2* and *psiCHECK-e4bp4-6*: the 3′UTRs of *aanat2* and *e4bp4-6* genes, containing binding recognition sites for miR-183, were cloned downstream to the *Renilla* luciferase open reading frame in psiCHECK-2 Vector (Promega) that includes a control *Firefly* luciferase reporter under a different promoter. A 680 bp fragment of *aanat2* 3′UTR was PCR-amplified from zebrafish embryo cDNA using specific primers (Supplementary Table S3E), both containing NotI restriction sites. The PCR product was digested with NotI and ligated into NotI-digested psiCHECK-2. A 2547 bp fragment of *e4bp4-6* 3′UTR was cloned into psiCHECK-2 in the same manner using specific primers (Supplementary Table S3E). *psiCHECK-aanat2-M183* and *psiCHECK-e4bp4-6-M183*: site-directed mutagenesis was used to specifically mutate 2 nt of the miR-183 seed site in *aanat2* 3′UTR and 3 nt of the miR-183 seed site in *e4bp4-6* 3′UTR, using QuikChange Site-directed mutagenesis kit (Stratagene) as instructed by the manufacturer. The sets of complementary primers used for generation of the desired point mutations are presented in Supplementary Table S3F. *miRVec-183*: the pre-miR-183 cloned into the miRNA expression vector (miRVec) was provided by Prof. R. Agami (36).

One day before transfection, HEK-293T cells were seeded in 96-well plates (Greiner Bio-One) at a density of 7500 cells per well, in Dulbecco's Modified Eagle Medium (Gibco BRL) supplemented with 10% fetal calf serum and 1% penicillin–streptomycin. Cells were transfected in quadruplicate using the jetPRIME Reagent (Polyplus-Transfection) according to the manufacturer's protocol, with 40 ng DNA: 4 ng psiCHECK-2 enclosing wild-type or mutated 3′UTR or an empty vector; 36 ng miRVec containing pre-miR-183 or an empty vector. Control wells were transfected with 40 ng pEGFP-1 vector (Clontech). 48 h after transfection, transfection efficiency was assessed by GFP fluorescence in control wells, and *Firefly* and *Renilla* luciferase activities were measured using the Dual-Luciferase Reporter Assay System kit (Promega) and a Veritas microplate luminometer (Turner BioSystems), according to the manufacturer's instructions. Co-transfection experiments were performed in three independent repeats.

aanat2 mRNA rhythm assay

The following procedure was designed to examine the effect of miR-183 knockdown on the *aanat2* mRNA rhythm in the pineal gland. Embryos were injected with control MO or miR-183$_{(guide)}$MO, exposed to two 12-h: 12-h LD cycles and sampled with 4-h intervals under DD during days 3–4 (CT2, 6, 10, 14, 18, 22 and 2b). Whole-mount ISH and quantification was conducted as formerly described (11) using the *aanat2* probe (37). This procedure was repeated twice.

RESULTS

Characterization of the light-responsive coding transcriptome in the zebrafish pineal gland

With the aim of identifying potential key players in light-entrainment of the circadian clock, we studied the effect of light exposure on gene expression in the zebrafish central clock organ, the pineal gland. Light-induced phase shifts of the clock are known to be time-of-day-dependent (38); therefore, it is likely that clock-related light-responses vary as a function of the circadian time. Taking this into account, the general experimental design included 1-h light treatments at six time points, evenly distributed throughout the daily cycle (Figure 1 and 'Materials and Methods' section). Characterization of the light-induced pineal gland transcriptome was carried out both by mRNA-seq and microarray analyses. mRNA-seq analysis was performed on triplicates of light and dark pineal gland samples that were pooled from six time points. Microarray analysis was conducted on six light and six dark pineal gland samples that were collected at 4-h intervals, thus providing information regarding the light-induction of genes at different circadian times.

The mRNA-seq analysis yielded a list of 92 light-induced genes in the pineal gland, which represent RefSeq-annotated genes (Table 1 and 'Materials and Methods' section). The microarray analysis revealed 29 light-induced RefSeq genes (Supplementary Table S1 and 'Materials and Methods' section). The higher number of light-induced genes detected by mRNA-seq reflects the limited gene representation on the microarrays and the enhanced precision of mRNA-seq in measurement of transcripts levels (16). Importantly, 19 (65%) of 29 RefSeq genes that were identified as light-induced by microarray were also detected by mRNA-seq.

A subset of genes was selected for validation by qRT-PCR on adult pineal glands or by whole-mount ISH in embryos (Figure 2), repeating the light and dark treatments as in the original experimental procedure (Figure 1 and 'Materials and Methods' section). The experimental validation of 9 of the 10 tested genes, together with the overlap between the two independent transcriptome methods, provides a high level of confidence for the identified light-induced genes.

Functional classification of light-regulated genes

The global impact of light exposure on biological processes was analyzed by DAVID annotation enrichment

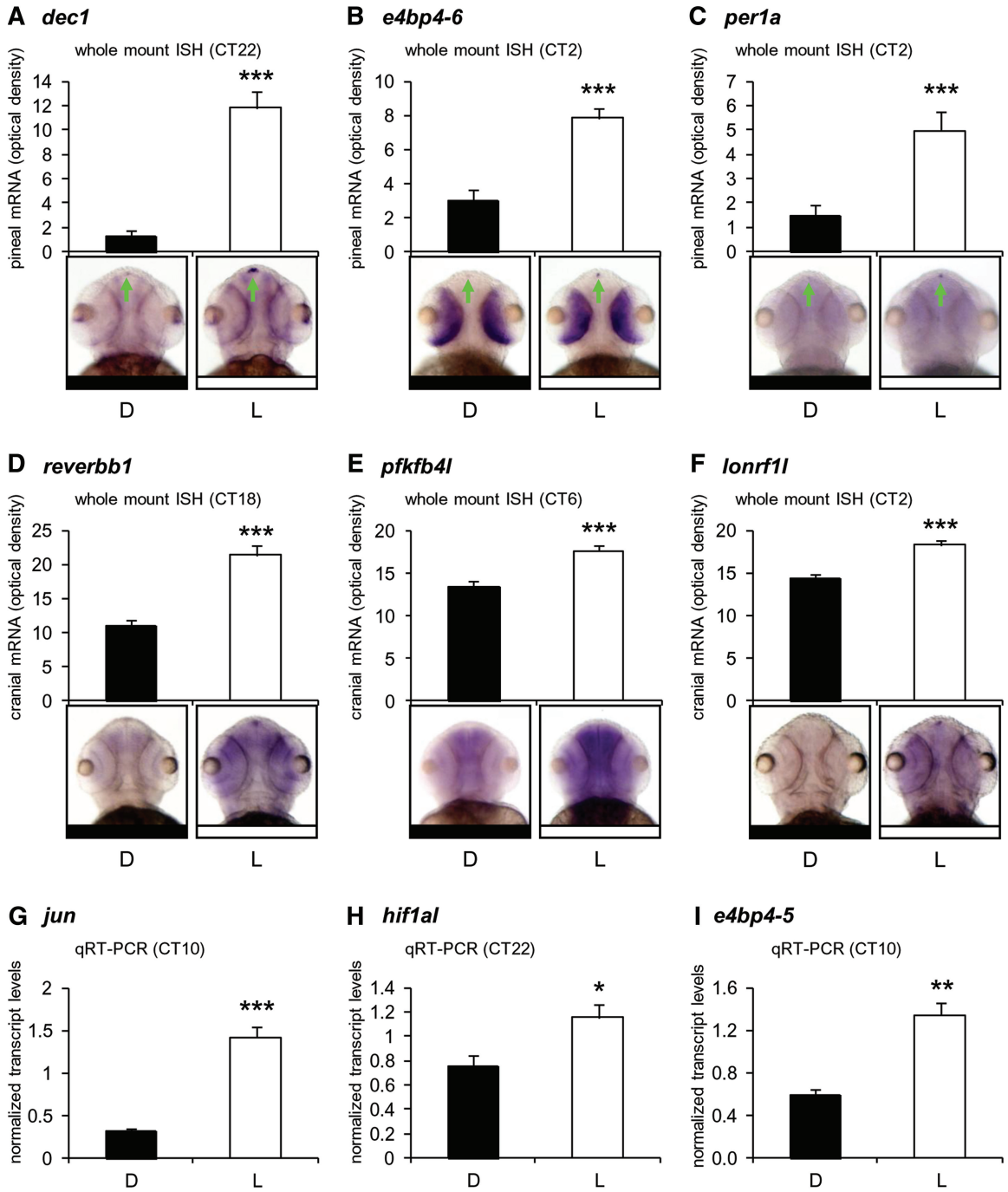

Figure 2. Validation of light-induction by whole-mount ISH and qRT-PCR. Upregulation of nine transcripts following 1-h of light (L) versus control darkness (D) is confirmed by quantitative whole-mount ISH on 48–72-h-old embryos (**A–F**) or by qRT-PCR on adult pineal gland samples (**G–I**). For ISH analysis, dorsal views of representative specimens are shown; signals in the pineal gland (A–C, green arrow) or the entire cranium area (D–F) were determined using ImageJ software. Error bars represent SE (A–F, $n = 15$–18; G–I, $n = 3$); $^{*}P < 0.05$, $^{**}P < 0.01$, $^{***}P < 0.001$, *t*-test. CT, circadian time.

tool (26). Significantly overrepresented Gene Ontology terms within the list of light-induced genes are listed in Supplementary Table S2 (Benjamini–Hochberg false discovery rate of 5%). Notably, multiple annotation terms associated with transcriptional regulation are significantly enriched (Supplementary Table S2), confirming the contribution of transcriptional control to the relay of photic information. An interesting finding is that ontology terms related to negative transcriptional regulation are highly represented (Supplementary Table S2), specifying the role of transcriptional repression in light signaling.

The enriched 'basic-leucine zipper domain' category supports a preferential role for basic-leucine zipper (bZIP) transcription factors in mediating light-regulated

gene expression. These include members of the PAR/E4BP4 bZIP subfamily and AP-1 transcription factor complex that have been functionally linked to the process of light-entrainment of the circadian clock (12,13,39).

Interestingly, Gene Ontology terms related to the response to reactive oxygen species (ROS), such as 'response to hydrogen peroxide', are significantly enriched, coinciding with the suggested involvement of ROS in light signaling (40).

Importantly, the most significantly enriched term is 'circadian rhythm - mammal' that consists of seven genes that are considered as orthologs of mammalian clock genes, some of which were not previously recognized as light regulated (see below and Table 2).

Circadian clock-related genes are induced by light

Light-induced transcription of the core clock genes *per2* and *cry1a* is well documented in most zebrafish tissues and cell lines and considered to play a fundamental role in the mechanism of clock entrainment by light (10,11). As mentioned above, additional clock gene orthologs that are induced by light in the pineal gland were identified by DAVID analysis. Furthermore, we identified several other light-induced clock accessory loop genes, bringing the total number of light-induced core clock and clock accessory loop genes in the pineal gland to 14 (Table 2). Besides *per2* and *cry1a*, two additional members of the negative limb of the core clock loop were encountered: *cry3*, which is also light-induced in zebrafish Pac-2 cells (15) and *per1a*. Transcriptional regulators belonging to clock accessory loops that were detected: *dec1* and *dec2*, basic helix-loop-helix (bHLH) transcription factors that repress CLOCK:BMAL-mediated transcription (41); *reverba*, *reverbb1* and *reverbb2*, members of the nuclear receptor (NR) family that contribute to the robustness of the clock mechanism by regulating the expression of core clock genes (42); *tef1*, *dbp2*, *e4bp4-2*, *e4bp4-5* and *e4bp4-6* belonging to the PAR/E4BP4 bZIP subfamily of clock-controlled genes that feedback onto the core clock (13,43–45). Confirming our results is the fact that some of the pineal light-induced genes (Table 2) were also identified previously, by microarray analyses, in other tissues or in cell lines (Supplementary Table S5).

Cellular metabolic pathways are induced by light

Hypoxia-inducible factor 1 alpha (*hif1a*) is a key player in the regulation of cellular adaptations to hypoxia. It is a PAS-domain bHLH transcription factor that binds to core DNA sequence within the hypoxia response element of target gene promoters (46). Previous studies established a cross-talk between hypoxic signaling and circadian pathways. In one case, the expression levels of the core clock components PER1 and CLOCK were increased in response to hypoxia in the mouse brain, an effect that was suggested to be mediated by direct interaction with HIF1a (47). In another example, a link between hypoxic and circadian pathways has been shown to exist in the combined transcriptional regulation of *vasopressin* by HIF1a and CLOCK via an E-box enhancer (48). Recently, evidence for the interaction between the two pathways have been demonstrated in zebrafish, including direct binding of HIF1a to E-boxes in the *per1* promoter, and both dampened *per1* circadian oscillations and loss of larval circadian activity patterns in response to hypoxia (49). In the present study, *hif1al* was identified and validated as being light-induced in the pineal gland (Table 1 and Figure 2H).

Interestingly, a well-characterized target of HIF1a (50), *pfkfb4* (*6-phosphofructo-2-kinase/fructose-2,6-biphosphatase*), an isoenzyme involved in regulation of glucose metabolism in response to hypoxia, is highly regulated by light in the pineal gland and cranial areas (Table 1 and Figure 2E). This gene exhibits the greatest L/D-fold expression according to both transcriptome analyses. The finding that *hif1al* and its target are upregulated by light, together with the established cross-talk between hypoxic and circadian pathways, suggests that the hypoxic pathway is activated by photic signaling and contributes to circadian clock entrainment.

Table 2. Circadian clock-related light-induced genes in the pineal gland, detected by mRNA-seq

Number	RefSeq ID	Gene symbol	Previous reports of light-induction in the zebrafish pineal gland
1	NM_001030183	*per1a*	
2	NM_182857	*per2*[a]	(11)
3	NM_001077297	*cry1a*	
4	NM_131786	*cry3*	
5	NM_212679	*bhlhe40 (dec1)*[a]	
6	NM_001039107	*bhlhe41 (dec2)*	
7	NM_205729	*nr1d1 (reverba)*	
8	NM_001130592	*nr1d2a (reverbb1)*[a]	
9	NM_131065	*nr1d2b (reverbb2)*	
10	NM_131400	*tefa (tef1)*	(13)
11	NM_001197062	*dbpb (dbp2)*	(27)
12	NM_001197065	*nfil3-2 (e4bp4-2)*	(27)
13	NM_001197058	*nfil3-5 (e4bp4-5)*[a]	(27)
14	NM_001002218	*nfil3-6 (e4bp4-6)*[a]	(27)

[a]Identified as light-induced in the pineal gland also by microarray analysis.

Differential effects of light-induced transcription factors on clock-controlled and light-driven promoter activation

The clock-related light-induced transcription factors, *dec1*, *reverbb1*, *e4bp4-5* and *e4bp4-6*, were selected for further analysis. The effects of these factors on clock- and light-regulated promoter activity were tested using the light-entrainable zebrafish cell line Pac-2 and a live-cell bioluminescence monitoring system. The *per1b-Luc* and *E-box$_{per1b}$-Luc* constructs are markers for clock-controlled expression (30), whereas expression of the luciferase reporter constructs *cry1a-Luc* and *D-box$_{per2}$-Luc* is primarily light-driven but with evidence for co-regulation by the circadian clock (12,13). Pac-2 cells were co-transfected with expression vectors for each of the tested transcription factors, together with the promoter/enhancer-reporter constructs, exposed to different lighting regimens, and luciferase activity was monitored

and compared with that of control-treated cells (Figure 3 and 'Materials and Methods' section).

Based on the luciferase activity values, it is evident that over-expression of *dec1* leads to a robust attenuation of the expression driven by the *per1b* promoter and E-box elements (Figure 3A). However, examination of the normalized luciferase activity levels reveals that the rhythmic expression patterns themselves were not abolished (Supplementary Figure S1). The attenuation of luciferase expression levels by *dec1* was not observed for D-box elements or a control non-rhythmic *AP-1-Luc* reporter, and only a moderate reduction of expression was evident for the *cry1a* promoter (Supplementary Figure S2). These effects of *dec1* could be attributed to repression of CLOCK:BMAL-induced transcription via E-box enhancers (41). Furthermore, *dec1* over-expression induced a phase delay of the rhythmic expression driven by the *cry1a* promoter and D-box elements under LD cycles ($P < 0.0001$, *t*-test), such that the anticipatory rise and decline of promoter activity were eliminated, as demonstrated by a peak at ~ZT12 (Figure 3A and Supplementary Table S4). This effect is presumably due to the repression of the clock machinery by *dec1*, leading to a predominantly light-induced expression pattern of the *cry1a* promoter and D-box elements, with an increase in expression during the light phase and a decrease during the dark phase, thus lacking the clock-generated anticipation of the light–dark and dark–light transitions.

Over-expression of *reverbb1* resulted in a decreased amplitude of the rhythms driven by the *per1b* promoter ($P < 0.0001$, *t*-test) and E-box elements ($P < 0.01$, *t*-test; Figure 3B and Supplementary Table S4), most likely due to repression of endogenous BMAL transcription by *reverbb1* through specific response element [RREs, (51)]. Moreover, *reverbb1* led to a phase shift of the rhythmic expression of D-box elements ($P < 0.001$, *t*-test) and, to a lesser extent, also of *cry1a* promoter-driven expression ($P < 0.01$, *t*-test; Figure 3B and Supplementary Table S4). This outcome resembles the effect induced by *dec1*, both resulting in a predominantly light-driven regulation as a consequence of an inhibited clock.

Interestingly, over-expression of *e4bp4-5* and *e4bp4-6* resulted in dissimilar effects. High levels of *e4bp4-6* led to disruption of the expression driven by D-box elements ($P < 0.0001$, *t*-test; Figure 3D and Supplementary Table S4), most likely due to its direct binding to D-box enhancers and transcriptional repression (52). However, *e4bp4-5* induced a lower amplitude of *per1b* promoter-driven rhythmic expression ($P < 0.05$, *t*-test; Supplementary Table S4), yet the expression pattern regulated by D-box elements remained rhythmic (Figure 3C). These results point to distinct functions for the two light-induced e4bp4 homologs, in which *e4bp4-6* is more related to light-regulation and *e4bp4-5* to general clock function.

Thus, constitutive over-expression of the four light-induced transcription factors resulted in differential effects on clock- and light-regulated expression in Pac-2 cells, demonstrating various mechanisms by which transcription factors can mediate light-input to the core clock machinery and modulate clock gene expression.

Light-induced genes are important for light-entrainment of rhythmic locomotor activity

per2, which was identified by our transcriptome analyses, has been shown to play a key role in the onset of the pineal clock *in vivo,* demonstrated by its importance in the establishment of the clock-controlled *aanat2* mRNA rhythm that is triggered by light pulses (11,33). We further studied the role of *per2 in vivo* by testing the effect of *per2* knockdown on the light-induced generation of clock-regulated behavior in larvae. Zebrafish larvae display circadian rhythms of locomotor activity characterized by a peak of activity during the subjective daytime (53). To entrain rhythms of locomotor activity, 5 dpf larvae were exposed to 3 h of light, and their locomotor activity was subsequently monitored under constant dim light conditions. The timing of the light pulse (beginning of the day or night) determined the peak time of locomotor activity rhythms (day or night, respectively), indicating that the light manipulation is responsible for the initiation of clock-controlled rhythmic activity and its entrainment (Supplementary Figure S3). *per2* knockdown [using *per2* morpholino, $per2_{(E4I4)}MO$] resulted in significantly disrupted patterns of circadian locomotor activity, as compared with control morpholino (cont MO)-injected embryos ($P < 0.001$; Figure 4A and C and 'Materials and Methods' section), demonstrating its role in light-entrainment of clock-regulated behavior.

We have shown that *dec1* is induced by light in the adult and larval pineal gland (Table 1 and Figure 2A). Light-induction of *dec1* has also been demonstrated in zebrafish larvae by microarray (15) and in the mouse SCN (41). The above experimental procedure was repeated to test the role of *dec1* in the light-induced onset of clock-driven locomotor activity. Knockdown of *dec1* [using *dec1* morpholino, $dec1_{(E2I2)}MO$] significantly affected the circadian locomotor activity patterns triggered by light pulses ($P < 0.0001$; Figure 4B and D and 'Materials and Methods' section). These results support our hypothesis that light-induction of *dec1* is important to the process of light-entrainment of the circadian clock. Together, these experiments demonstrate how the negative clock components, *dec1* and *per2*, which act at the central clock organ by different mechanisms, contribute to the light-entrainment of the circadian behavior.

Kinetics of light-dependent changes in mRNA levels

The kinetics of light-induced expression might provide important clues as to the position and function of genes in the light signaling cascades. Therefore, we determined the detailed time course of light-induction of *per2*, *cry1a*, *e4bp4-5*, *e4bp4-6* and *dec1* transcripts in the light-responsive Pac-2 cells. Following entrainment by three LD cycles, Pac-2 cells were kept in darkness or exposed to light and sampled at eight time periods. Transcript levels were determined by qRT-PCR (Figure 5). The expression of *per2*, *cry1a* and *e4bp4-6* was significantly affected by light treatment ($P < 0.0001$, two-way ANOVA) and sampling time ($P < 0.01$, two-way ANOVA). These transcripts display transient light-regulated expression patterns, in which mRNA levels rise following light

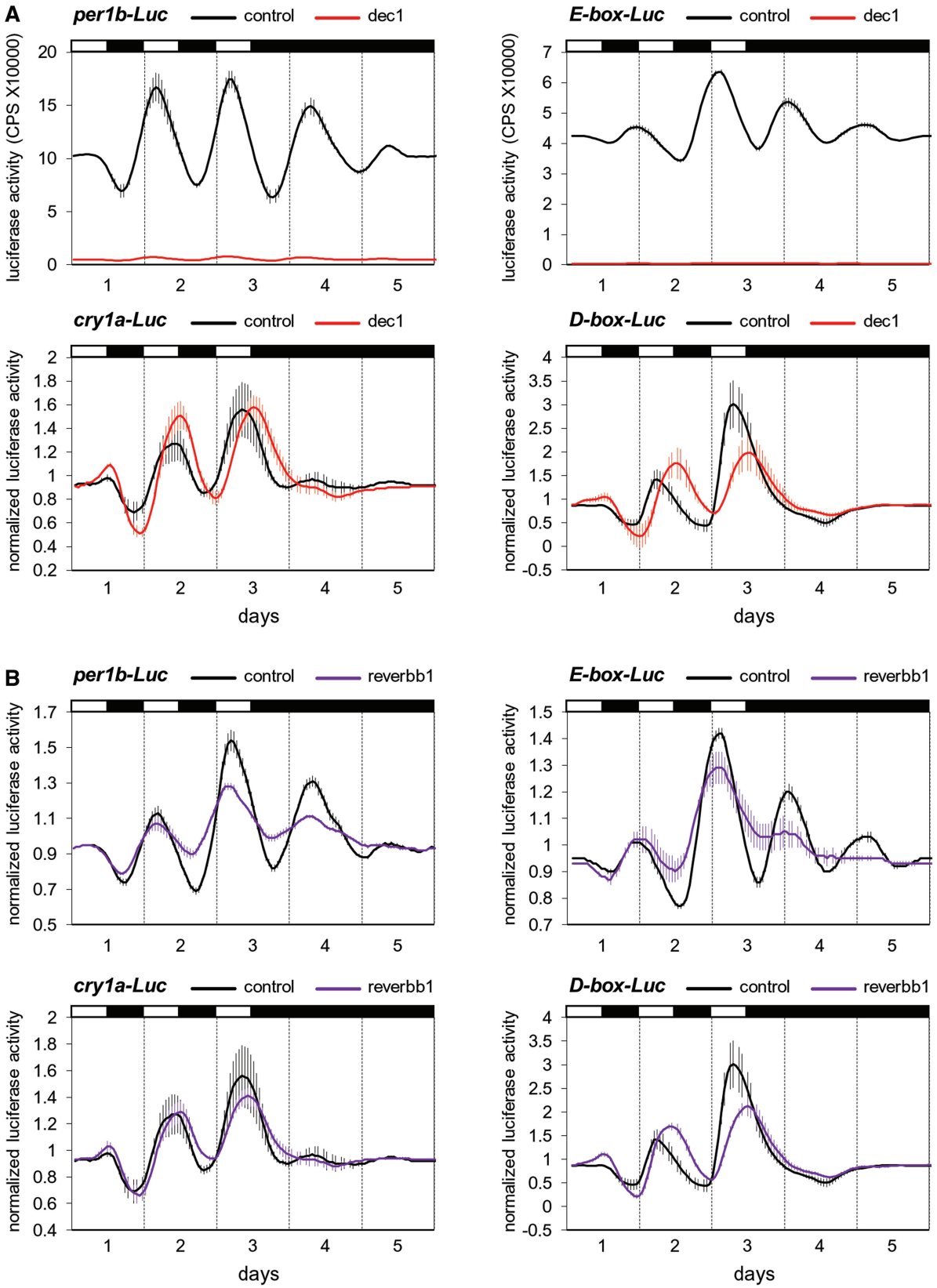

Figure 3. Light-induced transcription factors differentially affect clock- and light-regulated rhythmic promoter activity. Bioluminescence assay of zebrafish photosensitive Pac-2 cells transiently co-transfected with *dec1* (**A**), *reverbb1* (**B**), *e4bp4-5* (**C**) and *e4bp4-6* (**D**), together with *per1b-Luc* (A–D, top left), *E-box*$_{per1b}$*-Luc* (A–D, top right), *cry1a-Luc* (A–D, bottom left) and *D-box*$_{per2}$*-Luc* (A–D, bottom right). Normalized luciferase activity or luciferase activity values (counts per second, CPS) are plotted on the y-axis and time (days) is plotted on the x-axis. White and black bars above each panel represent the light and dark periods, respectively. Error bars represent SD.

(continued)

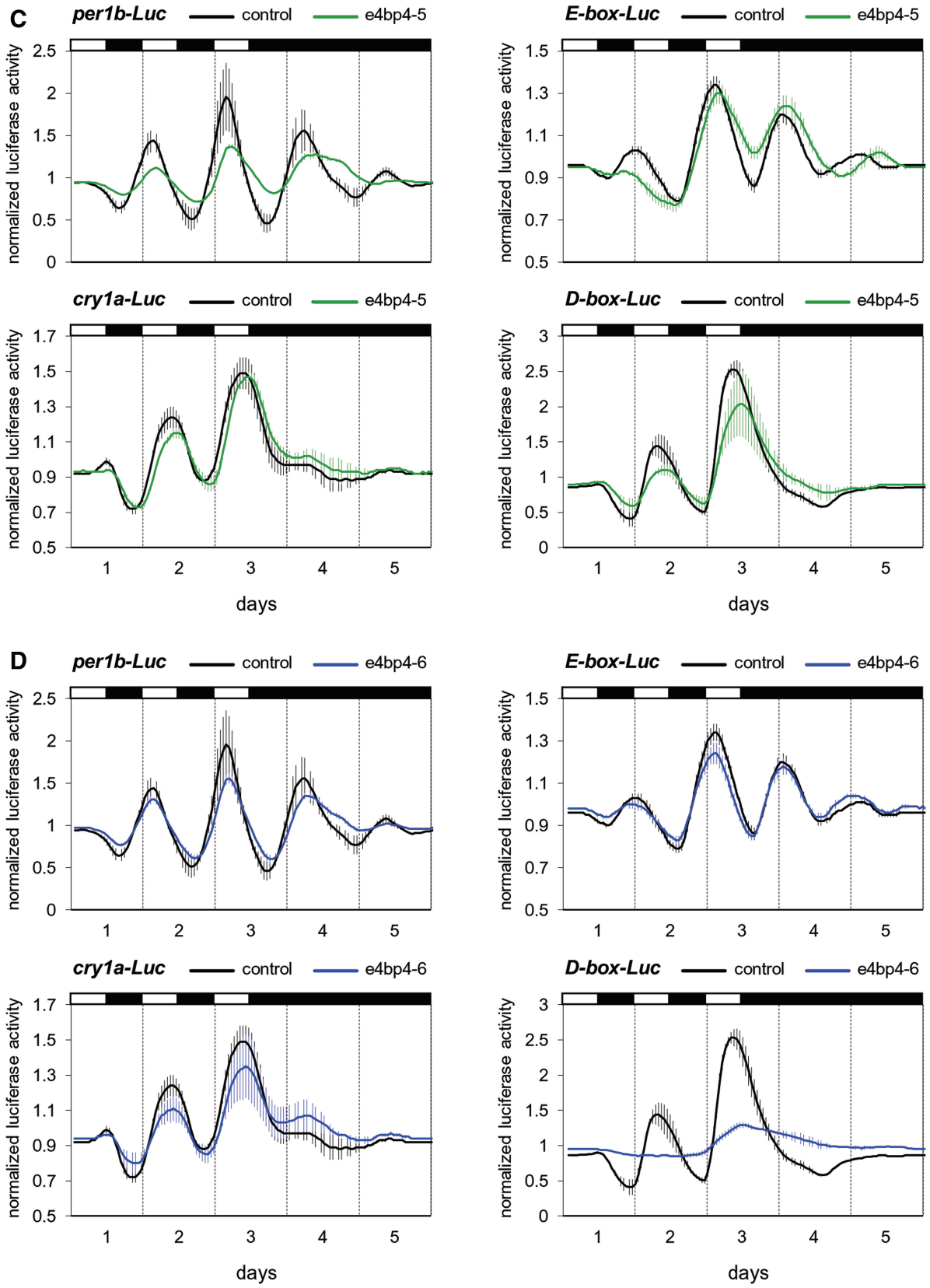

Figure 3. Continued

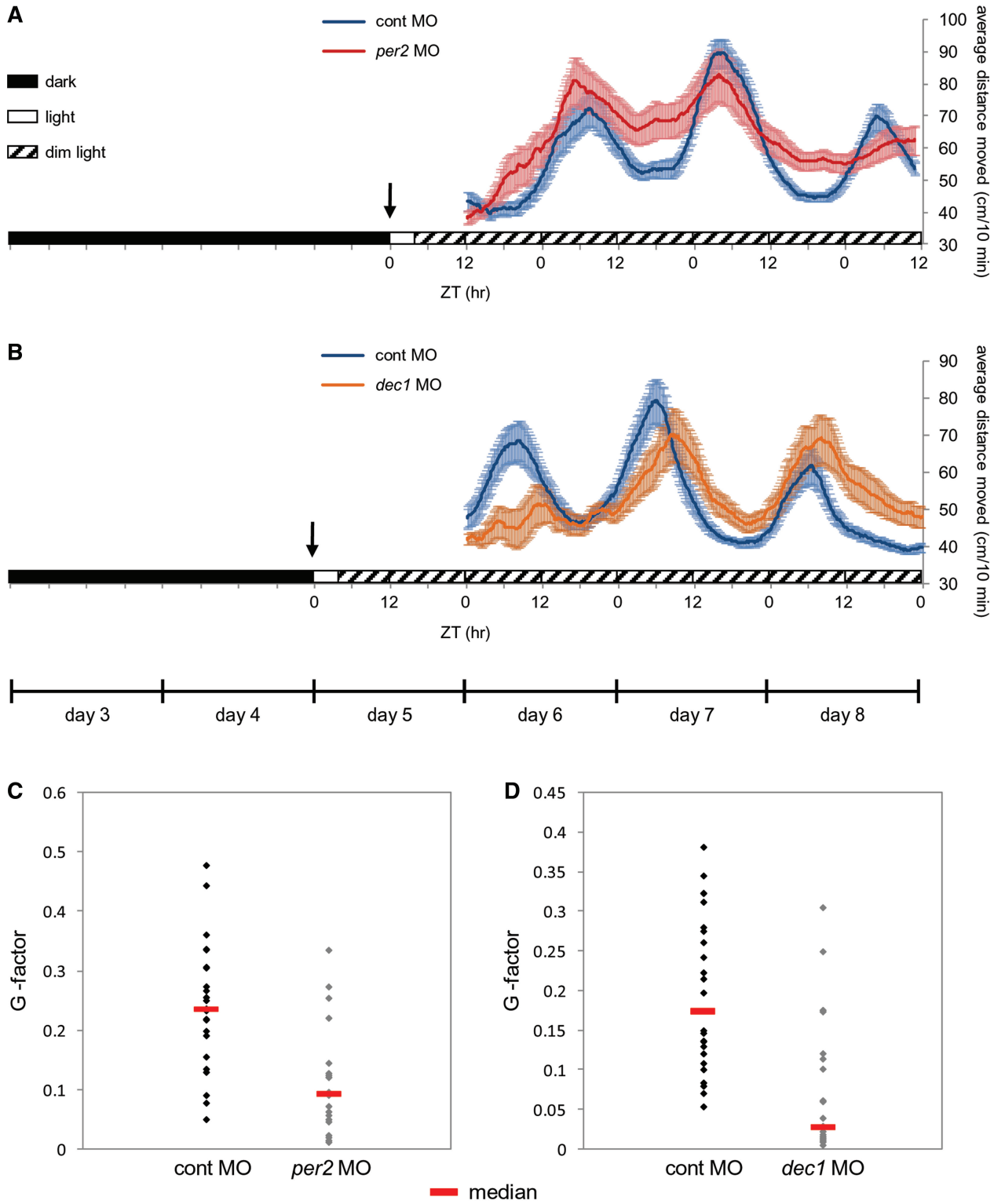

Figure 4. Knockdown of *per2* and *dec1* disrupts light-entrainment of rhythmic locomotor activity. Locomotor activity of 6–8 dpf larvae injected with control morpholino (cont MO; **A** and **B**, blue trendline), *per2* morpholino [per2$_{(E4I4)}$MO; A, red trendline] or *dec1* morpholino [dec1$_{(E2I2)}$MO; B, orange trendline] under constant conditions. Injected larvae were raised in constant darkness and entrained by 3-h light pulse (indicated by arrows) on day 5, which determined the phase and peak time of rhythmic locomotor activity as displayed by control larvae. The average distance moved (cm/10 min) is plotted on the y-axis and zeitgeber time (ZT) is plotted on the x-axis. Error bars stand for SE ($n = 24$). Horizontal boxes indicate the lighting conditions before and throughout activity monitoring: Black boxes represent dark, white boxes represents light and diagonally lined boxes represent dim light. Significant differences in the distribution of the G-factors (a representation of the extent to which the frequency of the activity pattern corresponds to a 24-h period, see 'larval locomotor activity assays' in 'Materials and Methods' section) were revealed between the control morpholino- (**C**, black diamonds) and *per2* morpholino (C, gray diamonds)-treated groups, as well as between the control morpholino- (**D**, black diamonds) and *dec1* morpholino (D, gray diamonds)-treated groups ($P < 0.001$ and < 0.0001, respectively). The median G-factor value for each group is indicated (C–D, red lines).

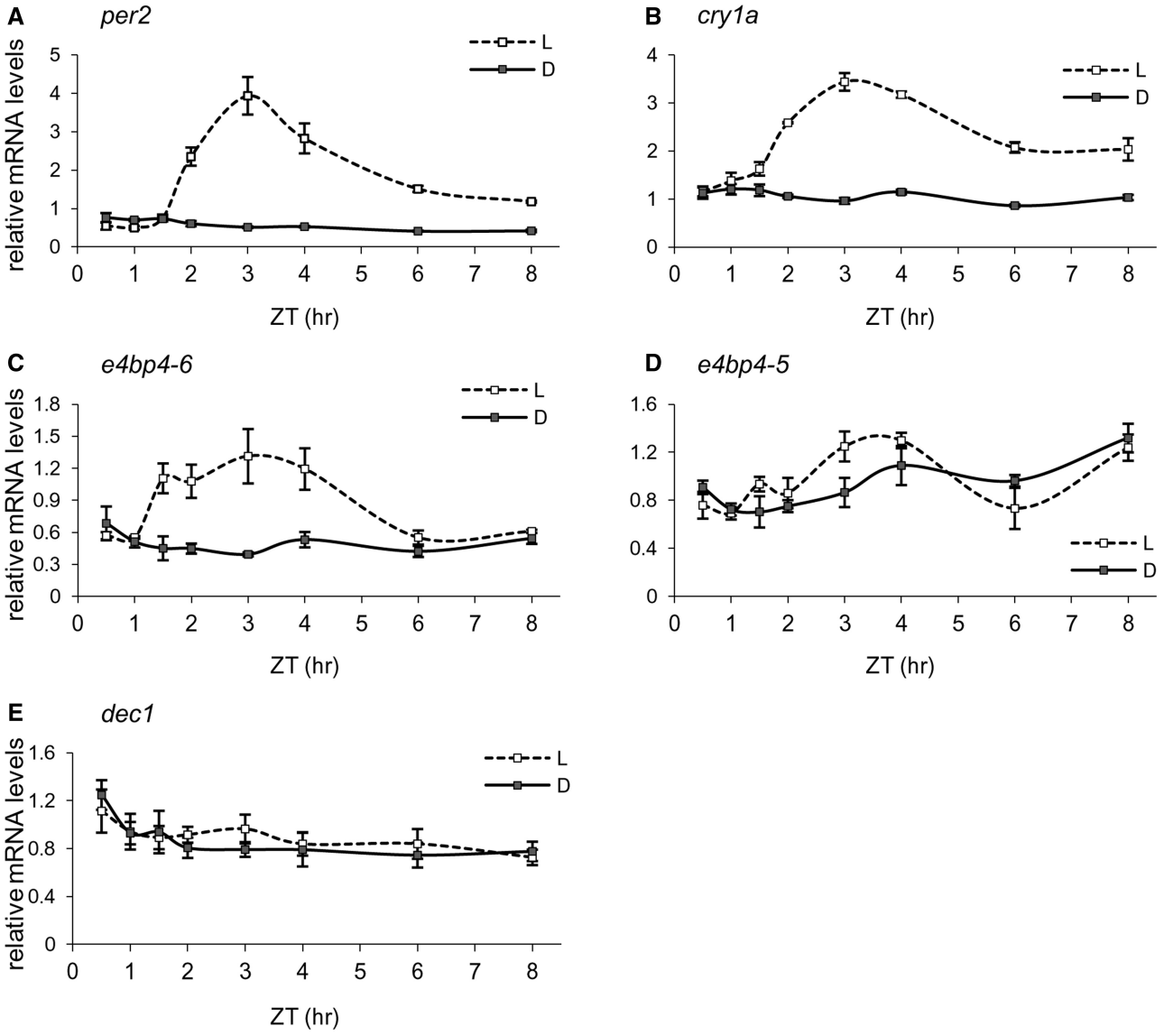

Figure 5. Time course of light-induction in Pac-2 cells. Cells were exposed to three LD cycles. Subsequently, total RNA was extracted from cells kept in darkness (filled boxes) or exposed to light (empty boxes) for different time periods (0.5, 1, 1.5, 2, 3, 4, 6 and 8 h). Quantification of *per2* (**A**), *cry1a* (**B**), *e4bp4-6* (**C**), *e4bp4-5* (**D**) and *dec1* (**E**) mRNA levels was performed by qRT-PCR. Values shown are the mean of three independent cell pools; error bars represent SE. Statistical differences between photic treatments and sampling times were determined by two-way ANOVA. ZT = zeitgeber time, ZT0 corresponds to the time of light onset.

onset, reach maximal levels within a few hours and gradually descend, comparing with low basal levels under dark conditions (Figure 5A–C). *e4bp4-6* mRNA is upregulated 1.5 h after light onset, slightly before *per2* induction, peaks at 3 h and gradually decays up to 6 h after light onset, similar to the *per2* transcript (Figure 5A and C). Together with the finding that *e4bp4-6* regulates the *per2* D-box (Figure 3D), these expression patterns suggest that *e4bp4-6* regulates *per2* light-induction. In contrast to *e4bp4-6*, the expression pattern of its homolog, *e4bp4-5*, is not light-regulated in Pac-2 cells (Figure 5D). Furthermore, unlike the case in the pineal gland, the *dec1* transcript is also not induced by light in Pac-2 cells (Figure 5E), consistent with a previous report in the zebrafish BRF41 cell line (54). Notably, the transient nature of the light-induction of genes, as demonstrated for *per2*, *cry1a* and *e4bp4-6*, is most likely essential for their function. These transient patterns of light-induction imply the existence of regulatory mechanisms governing the kinetics of mRNA degradation.

Pineal-enhanced and light-induced microRNAs

One regulatory mechanism that may contribute to the transient nature of the light-induced increase of specific transcripts involves targeting by miRNA. In the search for miRNAs that might be involved in circadian regulation and light-entrainment, miR-seq was used to profile the miRNA population whose expression is enriched in the pineal gland and is light-regulated ('Materials and Methods' section). Pineal glands were collected from

Table 3. The miR-183/96/182 cluster is pineal-enhanced and light-induced

miRNA	Pineal D[a]	Pineal L[a]	L/D-fold	Brain[a]	Pineal/brain-fold
dre-miR-182	4339677	7242855	1.67	2008	2884
dre-miR-96	4108	4735	1.15	5	908
dre-miR-183	114631	169606	1.48	178	800

[a]Normalized number of reads.

light- and dark-treated fish at six circadian times (Figure 1) and pooled together, generating 'light' and 'dark' samples. In addition, brains were collected from light- and dark-treated fish at CT2 and CT14 and pooled to generate a reference brain sample.

This analysis resulted in the identification of 32 miRNAs whose expression is enhanced in the pineal gland relative to the brain (Supplementary Table S6), and 31 miRNAs that are upregulated by light in the pineal gland (Supplementary Table S7). The overlap of these two sets consists of 14 miRNAs that exhibit pineal enhanced and light-induced expression (Supplementary Tables S6 and S7). Of particular interest is the miR-183/96/182 cluster that is highly enriched in the pineal gland and is also upregulated by light (Table 3). These findings are consistent with the abundance of this cluster in the rat pineal gland and retina (55) and with previous reports of light-regulation of this cluster in the mouse retina (56), thus pointing to a conserved function in vertebrates.

miR-183 targets the 3′UTR of the light-induced gene *e4bp4-6*

To identify potential targets of the pineal-enhanced and light-induced miR-183/96/182 cluster, we used TargetScanFish, a tool based on recognition site matching and features of site context [release 6.2, http://www.targetscan.org; (57)]. Focusing on predicted target genes that are characterized by a transient light-induced expression pattern, we selected *e4bp4-6*, which encloses a putative binding site for miR-183 in its 3′UTR, for further analysis. To test the ability of miR-183 to downregulate *e4bp4-6* mRNA levels, we used the luciferase reporter assay ('Materials and Methods' section). The 3′UTR of *e4bp4-6*, either with a wild-type sequence or carrying mutations in the miR-183 binding site (Figure 6B), was cloned downstream to a *Renilla* luciferase reporter gene. Reporter plasmids and miR-183 expression vector were co-transfected into HEK-293T cells. The relative activity of the *Renilla* luciferase reporters was normalized to control *Firefly* luciferase reporters and compared with control transfections with an empty miRNA expression vector. miR-183 significantly reduced the *Renilla* luciferase-*e4bp4-6* activity to 49%, compared with the control vector. However, when the miR-183 binding site was mutated the effect was statistically insignificant (Figure 6A). These results suggest that miR-183 may directly downregulate *e4bp4-6* mRNA levels by interacting with a target site in its 3′UTR. Furthermore, this finding serves as an example for the possible role of miRNAs in the generation of transient induction of transcripts in response to light, by promoting mRNA degradation.

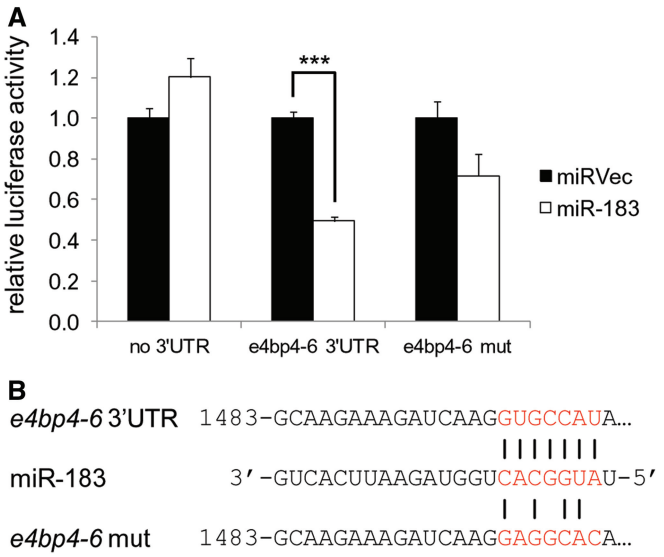

Figure 6. miR-183 regulates the *e4bp4-6* 3′UTR in HEK-293T cells. (**A**) miR-183 represses the luciferase activity of a *Renilla* reporter that harbors the wild-type *e4bp4-6* 3′UTR but not with mutated miR-183 target site (*e4bp4-6* mut) or empty reporter vector (no 3′UTR). Luciferase activity is normalized to the activity of *Firefly* luciferase co-expressed from the dual reporter and compared with a co-transfection of a negative control miRNA vector (miRVec). A representative experiment is shown. Error bars represent SE; ***$P < 0.001$, *t*-test with Bonferroni correction. (**B**) Representation of the miRNA–mRNA interaction tested in the luciferase assay, including the mutated miR-183 binding site.

miR-183 targets the 3′UTR of the clock-controlled gene *aanat2*

Subsequently, we asked whether light-induced miRNAs could also contribute to the generation of mRNA rhythms of clock-controlled genes. *aanat2* (*arylalkylamine-N-acetyltransferase-2*), the key enzyme in melatonin synthesis (58), is specifically expressed in the zebrafish pineal gland in a clock-dependent manner (37), and contains a potential target site for miR-183. We tested the direct interaction of miR-183 and its putative target site in *aanat2* 3′UTR using the luciferase reporter assay, as described in the previous section. A significant reduction of the *Renilla* luciferase activity (57%, compared with the control vector) was generated by miR-183 when the *aanat2* 3′UTR was included, an effect that was abolished when the miR-183 target site was mutated (Figure 7).

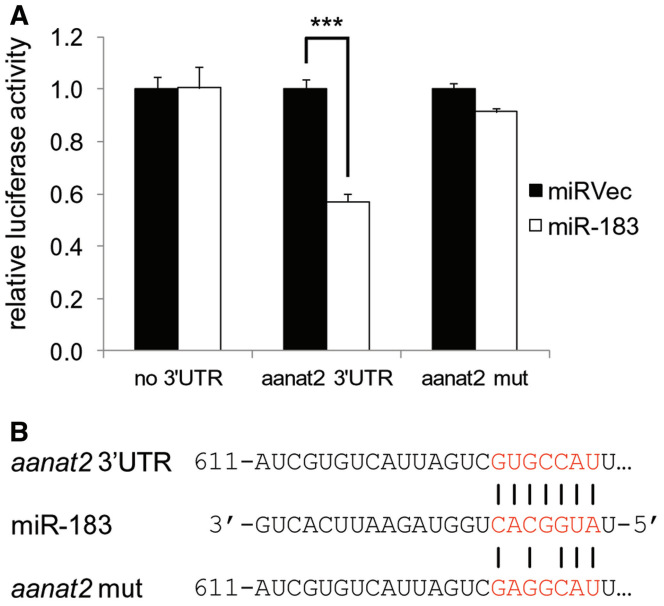

Figure 7. miR-183 regulates the *aanat2* 3′UTR in HEK-293T cells. (**A**) miR-183 represses the luciferase activity of a *Renilla* reporter that harbors the wild-type *aanat2* 3′UTR but not with mutated miR-183 target site (*aanat2* mut) or empty reporter vector (no 3′UTR). Luciferase activity is normalized to the activity of *Firefly* luciferase co-expressed from the dual reporter and compared with a co-transfection of a negative control miRNA vector (miRVec). A representative experiment is shown. Error bars represent SE; $***P < 0.001$, *t*-test with Bonferroni correction. (**B**) Representation of the miRNA–mRNA interaction tested in the luciferase assay, including the mutated miR-183 binding site.

This indicates that miR-183 might directly control *aanat2* mRNA levels through binding a target site in its 3′UTR, and adds support to the proposed involvement of miRNAs in the regulation of circadian mRNA rhythms (59).

miR-183 regulates pineal *aanat2* mRNA rhythms *in vivo*

To test whether miR-183 regulates *aanat2 in vivo*, we studied the effect of miR-183 morpholino-mediated knockdown on the rhythms of pineal gland *aanat2* mRNA levels. Zebrafish pineal *aanat2* transcription displays a robust circadian rhythm starting at 2 dpf (37). Morpholino-injected embryos were maintained under two LD cycles to entrain the circadian clock and then transferred to constant darkness. During the third and fourth days of development, embryos were collected at 4-h intervals and subjected to whole-mount ISH for *aanat2* mRNA. *aanat2* mRNA levels were significantly affected by morpholino treatment and sampling time ($P < 0.001$, two-way ANOVA). Specifically, miR-183 knockdown resulted in elevated *aanat2* mRNA levels compared with the control treatment at the end of the subjective night and beginning of subjective day (CT22 and CT2), time points at which a decline of *aanat2* mRNA normally occurs (Figure 8). These results suggest a role for miR-183 in the regulation of *aanat2* mRNA stability *in vivo* and its contribution to the rhythms of *aanat2* mRNA in the pineal gland.

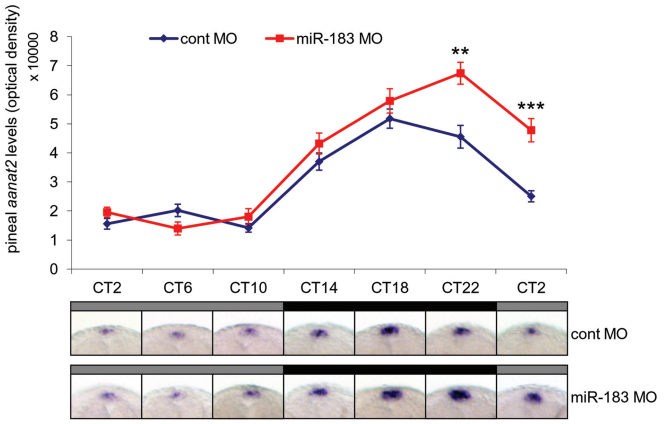

Figure 8. miR-183 knockdown effects the pineal *aanat2* mRNA rhythm. Zebrafish embryos were injected with control morpholino (cont MO) or miR-183 morpholino [miR-183$_{(guide)}$MO] and entrained by two LD cycles. On the third day of development, embryos were transferred to DD, sampled at 4-h intervals and pineal *aanat2* mRNA levels were determined by whole-mount ISH. Gray and black horizontal bars represent subjective day and night, respectively. Values represent the mean ± SE optical densities of the pineal signals ($n = 15$–20). Representative pineal *aanat2* signals (dorsal view) of embryos treated with cont MO (top panel) and miR-183$_{(guide)}$MO (bottom panel) from each group are presented. $**P < 0.01$, $***P < 0.001$, *t*-test with Bonferroni correction. CT, circadian time.

DISCUSSION

The zebrafish constitutes a fascinating vertebrate model for studying the regulation of the circadian clockwork by light (6). With the goal of further exploring the mechanisms underlying light-entrainment of the vertebrate circadian clock, we profiled the light-induced coding transcriptome and miRNome in the zebrafish central clock organ, the pineal gland, using cutting edge genome-wide methods.

An interesting outcome of this approach is the identification of 14 core clock and clock accessory loop genes that are induced by light in the pineal gland (Table 2). The finding of light-regulation of multiple clock components in a central clock tissue points to a complex regulatory mechanism underlying light-entrainment of the circadian clock. Notably, with the exception of two genes (*tef1* and *dbp2*), all these light-induced circadian clock-related genes function as transcriptional repressors, suggesting that light-entrainment is primarily mediated through the negative limbs of the oscillator. A similar result using microarray technology has been reported in the light-induced transcriptome of zebrafish larvae, heart and cell culture, in which six of the eight light-regulated clock genes that were identified act as transcriptional repressors (15). The functional analysis of selected light-regulated accessory loop genes (*dec1*, *reverbb1*, *e4bp4-5* and *e4bp4-6*) yielded differential effects on clock- and light-regulated expression in Pac-2 cells (Figure 3), demonstrating various mechanisms by which transcription factors modulate clock gene expression and thereby convey photic information to the core clock machinery.

The circadian clock regulator, *dec1*, strongly attenuated the clock-controlled expression driven by the *per1b*

promoter and E-box elements without affecting the phase (Figure 3A), probably reflecting its repression of CLOCK:BMAL-induced transcription (41). This repression of the clock machinery by *dec1* possibly underlies the elimination of the clock-derived anticipation in the *cry1a*- and D-box-driven expression, resulting in purely light-induced expression patterns (Figure 3A). We have shown that *dec1* is highly induced by light in the adult and larvae pineal gland (Table 1 and Figure 2A). This is also the case in the mouse SCN (41), but not in zebrafish cell lines [Figure 5E, (54)]. A study in *dec1*-deficient mice provided evidence for its role in circadian clock resetting (60). Our data indicate a similar role for *dec1* in the process of light-entrainment in zebrafish; knockdown of *dec1* resulted in disrupted circadian locomotor activity patterns that were triggered by a single light pulse (Figure 4B and D), resembling the effect generated by *per2* knockdown (Figure 4A and C). Light-induction of *per2* and *dec1* is predominant in the pineal gland. Nevertheless, whether the effects of these genes on entrainment of rhythmic behavior reflect their transcriptional effects and activities in the pineal gland or in peripheral clocks remains to be elucidated.

The D-box *cis*-acting element has been shown to serve a central role in light-driven gene expression in zebrafish (12,13,15). We have previously identified and characterized the zebrafish PAR/E4BP4 D-box binding factors (27). Here we show that two e4bp4 homologs, *e4bp4-5 and e4bp4-6*, both are induced by light in the pineal gland (Table 1 and Figure 2B and I), but only *e4bp4-6* is induced by light in Pac-2 cells (Figure 5C and D). Furthermore, these factors yielded differential effects on clock- and light-regulated promoter activation in Pac-2 cells (Figure 3C and D). In particular, *e4bp4-6* but not *e4bp4-5*, abolished expression driven by D-box elements, presumably by direct binding and transcriptional repression (52). Further studies will be required to assess the relative contribution of the various D-box-binding bZIP factors to the light response.

The transient nature of light-induced gene expression implies to the involvement of mechanisms that control mRNA stability, such as regulation by miRNA. In the search for candidate miRNAs that may play a role in light-entrainment and circadian regulation, the pineal gland-enhanced and light-induced miRNAs were profiled by miR-seq (Supplementary Tables S6 and S7). This analysis identified the miR-183/96/182 cluster, which is highly enriched in the pineal gland and upregulated by light (Table 3). This miRNA cluster has been formerly shown to exhibit a diurnal variation of expression in the mouse retina, and evidence were provided for their targeting of *adcy6*, a clock-controlled gene that modulates melatonin synthesis (61). In another study in the mouse retina, the miR-183/96/182 cluster was found to be light-regulated and to target the voltage-dependent glutamate transporter *slc1a1* (56). This cluster has also been shown to be abundantly expressed in the rat retina and pineal gland, where it displays daily dynamics of expression (55). Together, these findings suggest a conserved function for the miR-183/96/182 cluster in vertebrates and support its involvement in circadian and light-regulation. We have demonstrated that miR-183 downregulates *e4bp4-6* mRNA through a specific target site in its 3′UTR (Figure 6). Moreover, we have shown that miR-183 targets the 3′UTR (Figure 7) and regulates the rhythmic mRNA profile of the pineal clock-controlled gene, *aanat2*, *in vivo* (Figure 8). These findings emphasize the contribution of miRNAs to the transient expression profiles of light- and clock-regulated genes, and their importance to pineal functions, such as fine-tuning the kinetics of rhythmic melatonin production. Moreover, we have generated a database of additional miRNAs that may serve as candidates for regulating features of the vertebrate circadian clock and its entrainment by light.

The identity of the photopigments that mediate light-induction in the zebrafish pineal gland remains unclear, although several possible candidates have been suggested [as recently reviewed (6)]. Exo-rhodopsin as well as several other extra retinal opsins are expressed in the pineal gland and may act as photoreceptors (62–64). Another candidate opsin photoreceptor is teleost multiple tissue (TMT) opsin, whose mRNA is detected in the central nervous system, most peripheral tissues and even in cell lines (65) and has been confirmed to function as a photoreceptor (66). Consistently, most zebrafish tissues and even cell lines are directly light-responsive (8). CRYs were also suggested to act as photopigments due to the fact that CRY plays a role in photoreception by lateral neurons in *Drosophila* (67), and given that one of the zebrafish *cry* homologs (*cry4*) shares higher sequence similarity with *Drosophila cry* than with the mammalian homologs (68). Finally, light has been shown to induce the production of ROS such as H_2O_2 that might link photoreception to the induction of the zebrafish core clock genes *cry1a* and *per2* (40). It is suggested that light-activated enzymes such as flavin-containing oxidase function as photoreceptors that trigger accumulation of intracellular H_2O_2 upon exposure to near violet-blue wavelengths of light, as demonstrated in zebrafish Z3 cells (40). In addition, an interesting finding of the current study is that *hif1a*, as well as its characterized target *pfkfb4l*, are induced by light (Table 1 and Figure 2E and H). Together with observations of molecular cross-talk between hypoxic signaling and circadian pathways (47–49,69), these findings hint at the existence of an additional photic signaling cascade that might be involved in the process of light-entrainment. Any of the above photic transduction pathways may contribute to activating a set of light-induced genes in the pineal gland. The characterization of the light-induced transcriptome of the central clock organ points to the involvement of multiple pathways in the relay of photic information from photoreceptors to core circadian clock function.

The approach taken in this study enabled the identification of light-induced genes that may be involved in light-entrainment, the characterization of their action on the molecular clock and elucidating their effects on rhythmic behavior in the intact animal. Therefore, this study strengthens the utility of the zebrafish as a model for exploring the basic mechanisms whereby circadian clocks respond to the environment and how they have adapted during evolution.

SUPPLEMENTARY DATA

Supplementary Data are available at NAR Online.

ACKNOWLEDGEMENTS

The authors thank David C. Klein, Steven L. Coon and Reuven Stein for fruitful discussions.

FUNDING

The Israel Science Foundation [1084/12 to Y.G.]; the United States-Israel Binational Science Foundation [2009/290 to Y.G. and E.E.]; the Karlsruhe Institute of Technology (KIT, Germany) through the Helmholtz funding programme: BioInterfaces (to N.S.F.); and a scholarship from the Clore Israel Foundation (to S.A.). Funding for open access charge: The Israel Science Foundation [1084/12], Jerusalem, Israel.

Conflict of interest statement. None declared.

REFERENCES

1. Pittendrigh,C.S. (1993) Temporal organization: reflections of a Darwinian clock-watcher. *Annu. Rev. Physiol.*, **55**, 16–54.
2. Dunlap,J.C. (1999) Molecular bases for circadian clocks. *Cell*, **96**, 271–290.
3. Ko,C.H. and Takahashi,J.S. (2006) Molecular components of the mammalian circadian clock. *Hum. Mol. Genet.*, **15**, R271–R277.
4. Mehra,A., Baker,C.L., Loros,J.J. and Dunlap,J.C. (2009) Post-translational modifications in circadian rhythms. *Trends Biochem. Sci.*, **34**, 483–490.
5. Doyle,S. and Menaker,M. (2007) Circadian photoreception in vertebrates. *Cold Spring Harb. Symp. Quant. Biol.*, **72**, 499–508.
6. Vatine,G., Vallone,D., Gothilf,Y. and Foulkes,N.S. (2011) It's time to swim! zebrafish and the circadian clock. *FEBS Lett.*, **585**, 1485–1494.
7. Falcon,J., Besseau,L., Fuentes,M., Sauzet,S., Magnanou,E. and Boeuf,G. (2009) Structural and functional evolution of the pineal melatonin system in vertebrates. *Ann. N.Y. Acad. Sci.*, **1163**, 101–111.
8. Whitmore,D., Foulkes,N.S. and Sassone-Corsi,P. (2000) Light acts directly on organs and cells in culture to set the vertebrate circadian clock. *Nature*, **404**, 87–91.
9. Devlin,P.F. and Kay,S.A. (2001) Circadian photoperception. *Annu. Rev. Physiol.*, **63**, 677–694.
10. Tamai,T.K., Young,L.C. and Whitmore,D. (2007) Light signaling to the zebrafish circadian clock by Cryptochrome 1a. *Proc. Natl Acad. Sci. USA*, **104**, 14712–14717.
11. Ziv,L., Levkovitz,S., Toyama,R., Falcon,J. and Gothilf,Y. (2005) Functional development of the zebrafish pineal gland: light-induced expression of period2 is required for onset of the circadian clock. *J. Neuroendocrinol.*, **17**, 314–320.
12. Mracek,P., Santoriello,C., Idda,M.L., Pagano,C., Ben-Moshe,Z., Gothilf,Y., Vallone,D. and Foulkes,N.S. (2012) Regulation of per and cry genes reveals a central role for the D-Box enhancer in light-dependent gene expression. *PLoS One*, **7**, e51278.
13. Vatine,G., Vallone,D., Appelbaum,L., Mracek,P., Ben-Moshe,Z., Lahiri,K., Gothilf,Y. and Foulkes,N.S. (2009) Light directs zebrafish period2 expression via conserved D and E boxes. *PLoS Biol.*, **7**, e1000223.
14. Gavriouchkina,D., Fischer,S., Ivacevic,T., Stolte,J., Benes,V. and Dekens,M.P. (2010) Thyrotroph embryonic factor regulates light-induced transcription of repair genes in zebrafish embryonic cells. *PLoS One*, **5**, e12542.
15. Weger,B.D., Sahinbas,M., Otto,G.W., Mracek,P., Armant,O., Dolle,D., Lahiri,K., Vallone,D., Ettwiller,L., Geisler,R. *et al.* (2011) The light responsive transcriptome of the zebrafish: function and regulation. *PLoS One*, **6**, e17080.
16. Wang,Z., Gerstein,M. and Snyder,M. (2009) RNA-Seq: a revolutionary tool for transcriptomics. *Nat. Rev. Genet.*, **10**, 57–63.
17. Gothilf,Y., Toyama,R., Coon,S.L., Du,S.J., Dawid,I.B. and Klein,D.C. (2002) Pineal-specific expression of green fluorescent protein under the control of the serotonin-N-acetyltransferase gene regulatory regions in transgenic zebrafish. *Dev. Dyn.*, **225**, 241–249.
18. Trapnell,C., Pachter,L. and Salzberg,S.L. (2009) TopHat: discovering splice junctions with RNA-Seq. *Bioinformatics*, **25**, 1105–1111.
19. Levin,J.Z., Yassour,M., Adiconis,X., Nusbaum,C., Thompson,D.A., Friedman,N., Gnirke,A. and Regev,A. (2010) Comprehensive comparative analysis of strand-specific RNA sequencing methods. *Nat. Methods*, **7**, 709–715.
20. Alon,S., Vigneault,F., Eminaga,S., Christodoulou,D.C., Seidman,J.G., Church,G.M. and Eisenberg,E. (2011) Barcoding bias in high-throughput multiplex sequencing of miRNA. *Genome Res.*, **21**, 1506–1511.
21. Robinson,M.D. and Oshlack,A. (2010) A scaling normalization method for differential expression analysis of RNA-seq data. *Genome Biol.*, **11**, R25.
22. Alon,S., Mor,E., Vigneault,F., Church,G.M., Locatelli,F., Galeano,F., Gallo,A., Shomron,N. and Eisenberg,E. (2012) Systematic identification of edited microRNAs in the human brain. *Genome Res.*, **22**, 1533–1540.
23. Kozomara,A. and Griffiths-Jones,S. (2011) miRBase: integrating microRNA annotation and deep-sequencing data. *Nucleic Acids Res.*, **39**, D152–D157.
24. Bolstad,B.M., Irizarry,R.A., Astrand,M. and Speed,T.P. (2003) A comparison of normalization methods for high density oligonucleotide array data based on variance and bias. *Bioinformatics*, **19**, 185–193.
25. Rocke,D.M. and Durbin,B. (2001) A model for measurement error for gene expression arrays. *J. Comput. Biol.*, **8**, 557–569.
26. Huang da,W., Sherman,B.T. and Lempicki,R.A. (2009) Systematic and integrative analysis of large gene lists using DAVID bioinformatics resources. *Nat. Protoc.*, **4**, 44–57.
27. Ben-Moshe,Z., Vatine,G., Alon,S., Tovin,A., Mracek,P., Foulkes,N.S. and Gothilf,Y. (2010) Multiple PAR and E4BP4 bZIP transcription factors in zebrafish: diverse spatial and temporal expression patterns. *Chronobiol. Int.*, **27**, 1509–1531.
28. Lin,S., Gaiano,N., Culp,P., Burns,J.C., Friedmann,T., Yee,J.K. and Hopkins,N. (1994) Integration and germ-line transmission of a pseudotyped retroviral vector in zebrafish. *Science*, **265**, 666–669.
29. Vallone,D., Santoriello,C., Gondi,S.B. and Foulkes,N.S. (2007) Basic protocols for zebrafish cell lines: maintenance and transfection. *Methods Mol. Biol.*, **362**, 429–441.
30. Vallone,D., Gondi,S.B., Whitmore,D. and Foulkes,N.S. (2004) E-box function in a period gene repressed by light. *Proc. Natl Acad. Sci. USA*, **101**, 4106–4111.
31. Travnickova-Bendova,Z., Cermakian,N., Reppert,S.M. and Sassone-Corsi,P. (2002) Bimodal regulation of mPeriod promoters by CREB-dependent signaling and CLOCK/BMAL1 activity. *Proc. Natl Acad. Sci. USA*, **99**, 7728–7733.
32. Abe,M., Herzog,E.D., Yamazaki,S., Straume,M., Tei,H., Sakaki,Y., Menaker,M. and Block,G.D. (2002) Circadian rhythms in isolated brain regions. *J. Neurosci.*, **22**, 350–356.
33. Ziv,L. and Gothilf,Y. (2006) Circadian time-keeping during early stages of development. *Proc. Natl Acad. Sci. USA*, **103**, 4146–4151.
34. Smadja Storz,S., Tovin,A., Mracek,P., Alon,S., Foulkes,N.S. and Gothilf,Y. (2013) Casein kinase 1delta activity: a key element in the zebrafish circadian timing system. *PLoS One*, **8**, e54189.
35. Tovin,A., Alon,S., Ben-Moshe,Z., Mracek,P., Vatine,G., Foulkes,N.S., Jacob-Hirsch,J., Rechavi,G., Toyama,R., Coon,S.L. *et al.* (2012) Systematic identification of rhythmic genes reveals camk1gb as a new element in the circadian clockwork. *PLoS Genet.*, **8**, e1003116.
36. Voorhoeve,P.M., le Sage,C., Schrier,M., Gillis,A.J., Stoop,H., Nagel,R., Liu,Y.P., van Duijse,J., Drost,J., Griekspoor,A. *et al.*

(2006) A genetic screen implicates miRNA-372 and miRNA-373 as oncogenes in testicular germ cell tumors. *Cell*, **124**, 1169–1181.
37. Gothilf,Y., Coon,S.L., Toyama,R., Chitnis,A., Namboodiri,M.A. and Klein,D.C. (1999) Zebrafish serotonin N-acetyltransferase-2: marker for development of pineal photoreceptors and circadian clock function. *Endocrinology*, **140**, 4895–4903.
38. Duffy,J.F. and Wright,K.P. Jr. (2005) Entrainment of the human circadian system by light. *J. Biol. Rhythms*, **20**, 326–338.
39. Hirayama,J., Cardone,L., Doi,M. and Sassone-Corsi,P. (2005) Common pathways in circadian and cell cycle clocks: light-dependent activation of Fos/AP-1 in zebrafish controls CRY-1a and WEE-1. *Proc. Natl Acad. Sci. USA*, **102**, 10194–10199.
40. Hirayama,J., Cho,S. and Sassone-Corsi,P. (2007) Circadian control by the reduction/oxidation pathway: catalase represses light-dependent clock gene expression in the zebrafish. *Proc. Natl Acad. Sci. USA*, **104**, 15747–15752.
41. Honma,S., Kawamoto,T., Takagi,Y., Fujimoto,K., Sato,F., Noshiro,M., Kato,Y. and Honma,K. (2002) Dec1 and Dec2 are regulators of the mammalian molecular clock. *Nature*, **419**, 841–844.
42. Teboul,M., Guillaumond,F., Grechez-Cassiau,A. and Delaunay,F. (2008) The nuclear hormone receptor family round the clock. *Mol. Endocrinol.*, **22**, 2573–2582.
43. Doi,M., Nakajima,Y., Okano,T. and Fukada,Y. (2001) Light-induced phase-delay of the chicken pineal circadian clock is associated with the induction of cE4bp4, a potential transcriptional repressor of cPer2 gene. *Proc. Natl Acad. Sci. USA*, **98**, 8089–8094.
44. Ohno,T., Onishi,Y. and Ishida,N. (2007) A novel E4BP4 element drives circadian expression of mPeriod2. *Nucleic Acids Res.*, **35**, 648–655.
45. Yamaguchi,S., Mitsui,S., Yan,L., Yagita,K., Miyake,S. and Okamura,H. (2000) Role of DBP in the circadian oscillatory mechanism. *Mol. Cell. Biol.*, **20**, 4773–4781.
46. Semenza,G.L. (1998) Hypoxia-inducible factor 1: master regulator of O2 homeostasis. *Curr. Opin. Genet. Dev.*, **8**, 588–594.
47. Chilov,D., Hofer,T., Bauer,C., Wenger,R.H. and Gassmann,M. (2001) Hypoxia affects expression of circadian genes PER1 and CLOCK in mouse brain. *FASEB J.*, **15**, 2613–2622.
48. Ghorbel,M.T., Coulson,J.M. and Murphy,D. (2003) Cross-talk between hypoxic and circadian pathways: cooperative roles for hypoxia-inducible factor 1alpha and CLOCK in transcriptional activation of the vasopressin gene. *Mol. Cell. Neurosci.*, **22**, 396–404.
49. Egg,M., Koblitz,L., Hirayama,J., Schwerte,T., Folterbauer,C., Kurz,A., Fiechtner,B., Most,M., Salvenmoser,W., Sassone-Corsi,P. *et al.* (2013) Linking oxygen to time: the bidirectional interaction between the hypoxic signaling pathway and the circadian clock. *Chronobiol. Int.*, **30**, 510–529.
50. Minchenko,O., Opentanova,I., Minchenko,D., Ogura,T. and Esumi,H. (2004) Hypoxia induces transcription of 6-phosphofructo-2-kinase/fructose-2,6-biphosphatase-4 gene via hypoxia-inducible factor-1alpha activation. *FEBS Lett.*, **576**, 14–20.
51. Guillaumond,F., Dardente,H., Giguere,V. and Cermakian,N. (2005) Differential control of Bmal1 circadian transcription by REV-ERB and ROR nuclear receptors. *J. Biol. Rhythms*, **20**, 391–403.
52. Cowell,I.G. (2002) E4BP4/NFIL3, a PAR-related bZIP factor with many roles. *Bioessays*, **24**, 1023–1029.
53. Cahill,G.M., Hurd,M.W. and Batchelor,M.M. (1998) Circadian rhythmicity in the locomotor activity of larval zebrafish. *Neuroreport*, **9**, 3445–3449.
54. Abe,T., Ishikawa,T., Masuda,T., Mizusawa,K., Tsukamoto,T., Mitani,H., Yanagisawa,T., Todo,T. and Iigo,M. (2006) Molecular analysis of Dec1 and Dec2 in the peripheral circadian clock of zebrafish photosensitive cells. *Biochem. Biophys. Res. Commun.*, **351**, 1072–1077.
55. Clokie,S.J., Lau,P., Kim,H.H., Coon,S.L. and Klein,D.C. (2012) MicroRNAs in the pineal gland: miR-483 regulates melatonin synthesis by targeting arylalkylamine n-acetyltransferase. *J. Biol. Chem.*, **287**, 25312–25324.
56. Krol,J., Busskamp,V., Markiewicz,I., Stadler,M.B., Ribi,S., Richter,J., Duebel,J., Bicker,S., Fehling,H.J., Schubeler,D. *et al.* (2010) Characterizing light-regulated retinal microRNAs reveals rapid turnover as a common property of neuronal microRNAs. *Cell*, **141**, 618–631.
57. Ulitsky,I., Shkumatava,A., Jan,C.H., Subtelny,A.O., Koppstein,D., Bell,G.W., Sive,H. and Bartel,D.P. (2012) Extensive alternative polyadenylation during zebrafish development. *Genome Res.*, **22**, 2054–2066.
58. Klein,D.C. (2007) Arylalkylamine N-acetyltransferase: "the Timezyme". *J. Biol. Chem.*, **282**, 4233–4237.
59. Mehta,N. and Cheng,H.Y. (2012) Micro-managing the circadian clock: the role of microRNAs in biological timekeeping. *J. Mol. Biol.*, **425**, 3609–3624.
60. Rossner,M.J., Oster,H., Wichert,S.P., Reinecke,L., Wehr,M.C., Reinecke,J., Eichele,G., Taneja,R. and Nave,K.A. (2008) Disturbed clockwork resetting in Sharp-1 and Sharp-2 single and double mutant mice. *PLoS One*, **3**, e2762.
61. Xu,S., Witmer,P.D., Lumayag,S., Kovacs,B. and Valle,D. (2007) MicroRNA (miRNA) transcriptome of mouse retina and identification of a sensory organ-specific miRNA cluster. *J. Biol. Chem.*, **282**, 25053–25066.
62. Pierce,L.X., Noche,R.R., Ponomareva,O., Chang,C. and Liang,J.O. (2008) Novel functions for Period 3 and Exo-rhodopsin in rhythmic transcription and melatonin biosynthesis within the zebrafish pineal organ. *Brain Res.*, **1223**, 11–24.
63. Toyama,R., Chen,X., Jhawar,N., Aamar,E., Epstein,J., Reany,N., Alon,S., Gothilf,Y., Klein,D.C. and Dawid,I.B. (2009) Transcriptome analysis of the zebrafish pineal gland. *Dev Dyn.*, **238**, 1813–1826.
64. Ziv,L., Tovin,A., Strasser,D. and Gothilf,Y. (2007) Spectral sensitivity of melatonin suppression in the zebrafish pineal gland. *Exp. Eye Res.*, **84**, 92–99.
65. Moutsaki,P., Whitmore,D., Bellingham,J., Sakamoto,K., David-Gray,Z.K. and Foster,R.G. (2003) Teleost multiple tissue (tmt) opsin: a candidate photopigment regulating the peripheral clocks of zebrafish? *Brain Res. Mol. Brain Res.*, **112**, 135–145.
66. Cavallari,N., Frigato,E., Vallone,D., Frohlich,N., Lopez-Olmeda,J.F., Foa,A., Berti,R., Sanchez-Vazquez,F.J., Bertolucci,C. and Foulkes,N.S. (2011) A blind circadian clock in cavefish reveals that opsins mediate peripheral clock photoreception. *PLoS Biol.*, **9**, e1001142.
67. Ceriani,M.F., Darlington,T.K., Staknis,D., Mas,P., Petti,A.A., Weitz,C.J. and Kay,S.A. (1999) Light-dependent sequestration of TIMELESS by CRYPTOCHROME. *Science*, **285**, 553–556.
68. Kobayashi,Y., Ishikawa,T., Hirayama,J., Daiyasu,H., Kanai,S., Toh,H., Fukuda,I., Tsujimura,T., Terada,N., Kamei,Y. *et al.* (2000) Molecular analysis of zebrafish photolyase/cryptochrome family: two types of cryptochromes present in zebrafish. *Genes Cells*, **5**, 725–738.
69. Hogenesch,J.B., Gu,Y.Z., Jain,S. and Bradfield,C.A. (1998) The basic-helix-loop-helix-PAS orphan MOP3 forms transcriptionally active complexes with circadian and hypoxia factors. *Proc. Natl Acad. Sci. USA*, **95**, 5474–5479.